1-1-1975

Semiclassical Calculation of Regge Poles

J. B. Delos
William & Mary, jbdelo@wm.edu

C. E. Carlson

Recommended Citation

Delos, J. B. and Carlson, C. E., Semiclassical Calculation of Regge Poles (1975). *Physical Review A*, 11(1). 10.1103/PhysRevA.11.210

Semiclassical calculation of Regge poles

J. B. Delos and C. E. Carlson
Department of Physics, College of William and Mary, Williamsburg, Virginia 23185
(Received 11 June 1974)

We have calculated the locations of the Regge poles for an actual interatomic potential by following the semiclassical formulation. For negative energies, this formulation is equivalent to the Bohr-Sommerfeld quantization condition. For positive energies there are three complex turning points; use of linear and parabolic connection formulas yields a semiclassical quantization condition for the poles. The poles are found to lie symmetrically along lines in the first and third quadrants of the angular-momentum plane. The locations of the poles at a given energy and the motion of these poles as the energy changes are presented. Remler has shown that Regge poles provide a convenient way of parametrizing experimental differential cross sections. We discuss the relation between this parametrization and the present results.

I. INTRODUCTION

In this paper we present a calculation of the locations of the Regge poles of an actual interatomic potential. Regge poles have been applied widely in high-energy physics, but are not in general use in atomic studies. However, in recent years, the Regge-pole idea has proved to be practical for describing elastic atom-atom scattering.[1,2] The advantage of this description is the same advantage that led Watson and Sommerfeld[3] to develop the technique for a different problem: In certain circumstances it provides important simplifications. The conventional partial-wave description of scattering is adequate, but tedious because hundreds (or sometimes thousands) of partial waves are needed. However, by a suitable transformation, the sum over partial waves may be replaced by a shorter sum involving Regge poles. Among the advantages are that there are fewer parameters and that the parameters are closely related to the observed features in the differential cross section.

The standard partial wave sum may be written as

$$f(\theta)=\frac{1}{2ik}\sum_L (2L+1)(e^{2i\delta_L}-1)P_L(\cos\theta),$$

where δ_L is the phase shift, and S-matrix elements are given by $S=e^{2i\delta_L}$. Watson and Sommerfeld noted that if one considers the summand to be a continuous function of complex L, and multiplies it by $\sec(L+\frac{1}{2})$, then the sum is exactly equivalent to an integral around a contour that encloses the positive real L axis. Further, if the S-matrix element is analytic except for isolated poles in the first quadrant, the contour can be deformed to lie along the imaginary L axis. Then the scattering amplitude is obtained from this "background" integral and the residues of the poles of the S matrix in the first quadrant. This transformation is useful if the scattering amplitude is dominated by a relatively simple sum over a few poles.

Remler has recently shown that this approach is very useful in analyzing low-energy (few eV) ion-atom differential scattering experiments. The approximations he made suggest the hypothesis that the important poles lie in a cluster in the complex L plane. The S matrix was written in a manifestly unitary form, and for reasons that shall be made clear, was made symmetric in the variable $\lambda=L+\frac{1}{2}$:

$$S=\prod_P \frac{\lambda^2-\lambda_P^{*2}}{\lambda^2-\lambda_P^2}.$$

We can understand Remler's hypothesis by considering the classical deflection function $\Theta(L)=2\,d\delta/dL$. Figure 1 shows a deflection function for a typical atomic-scattering process, and also the deflection function calculated from a single Regge pole. The attractive portion of the deflection function can be approximated by a deflection function obtained from a cluster of poles at a point λ_P in the complex λ plane. The rainbow angle Θ_R, its location λ_R, and the full width Γ of the deflection function at $\Theta=\frac{1}{2}\Theta_R$ are connected to the number of poles N and pole position λ_P by

$$\Theta_R\simeq 2N/\mathrm{Im}\lambda_P,\quad \lambda_R=\mathrm{Re}\lambda_P,\quad \Gamma=2\,\mathrm{Im}\lambda_P.$$

Thus, as described by Bobbio, Rich, Champion, and Doverspike,[2] the pole parameters can be fairly well approximated by an inspection of the experimental data. (The repulsive scattering is most conveniently accounted for by explicitly including a short-range core.) The differential cross section may then be calculated, and with some adjustment of the parameters excellent agreement between experiment and calculation is achieved.

The Regge-Remler parametrization of the differential cross section has, in particular, been

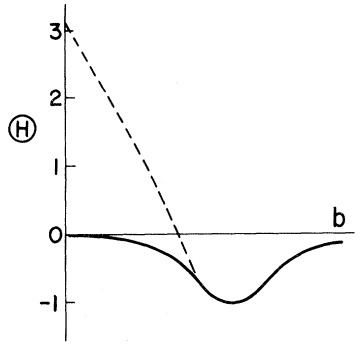

FIG. 1. Deflection function. The solid line is the attractive part of the deflection function, which can be represented by Regge poles in the first quadrant.

effective as an intermediary in the semiclassical inverse-scattering problem, which deals with procedures for obtaining interatomic potentials from scattering data. The inversion proceeds straightforwardly once the phase shifts are known as a function of L. It is hard to solve for the phase shifts directly from the data. On the other hand, it is not hard to find the Regge pole parameters, and from the S matrix thus obtained, to solve for the phase shifts and then the potential.

In this paper we will calculate in the reverse direction. We take a realistic interatomic potential and find the locations and residues of the poles of the S-matrix that it generates. Specifically, the potentials we study are analytic approximations to the potential for H^+Ar elastic scattering. We use a semiclassical treatment, developed in this context by Connor,[4] to obtain a relation between the pole position and relevant integrals involving the potential. This relation may be thought of as an extension of the Bohr-Sommerfeld quantization condition for bound states. Since several potentials (Yukawa, Coulomb, repulsive hard core) have had their Regge structure delineated[5] and show lines of poles rather than clusters, we wished to see how the actual poles compared to the cluster hypothesis. Also, we wished to understand why the cluster hypothesis does give such good fits to the data.

A further review of Regge theory is given briefly in Sec. II. The outline of the derivation of the semiclassical Regge quantization condition is given in Sec. III, and the resulting Regge poles are displayed in Sec. IV. Comments and conclusions appear in Sec. V.

II. GENERAL THEORY

A. Definitions and notation

Elastic scattering is described by the Schrödinger equation

$$[-(\hbar^2/2M)\nabla^2 + V(R)]\,\Psi(\vec{R}) = E\Psi(\vec{R}). \tag{1}$$

With the usual expansion in partial waves,

$$\Psi(\vec{R}) = \sum_L c_L[u_L(R)/R]P_L(\cos\Theta) \tag{2}$$

together with the Langer modification, we obtain the radial Schrödinger equation

$$\left(-\frac{\hbar^2}{2M}\frac{d^2}{dR^2} + V(R) + \frac{(L+\frac{1}{2})^2}{2MR^2}\right)u_L(R) = Eu_L(R). \tag{3}$$

The boundary conditions for the regular solutions are

$$u_L(R) \xrightarrow{R\to 0} 0, \tag{4a}$$

$$u_L(R) \xrightarrow{R\to\infty} e^{-ikR} + (-1)^{L+1}S_L e^{ikR}. \tag{4b}$$

The S "matrix," defined by Eq. (4) for positive integer L and real E, can be analytically continued into the complex L plane; we shall always consider E to be real. With suitable restrictions on $V(R)$, one can prove that $S(L)$ is a meromorphic function at least in the right half-plane, having only isolated poles. These poles occur at values of L where $u_L(R)$ (by definition bounded at the origin) has no asymptotic incoming part. It is well known that these poles may represent bound states or resonant states; to some extent the same poles also might describe rainbow scattering.

B. Symmetry

The Schrödinger equation depends only on $(L+\frac{1}{2})^2$, and not on L itself; accordingly, it might be suspected that the positions of the Regge poles would be symmetric in $\lambda = L+\frac{1}{2}$. However, this is not true in general. If the potential $V(R)$ is less singular than $1/r^2$ at the origin, then the effective potential near $R=0$ is dominated by the centrifugal term, and the boundary condition (4a) on the regular solution is

$$u_L(R) \to R^L.$$

This is only appropriate if $\mathrm{Re}\lambda > 0$, and one can go from $\mathrm{Re}\lambda > 0$ to $\mathrm{Re}\lambda < 0$ only by a careful process of analytic continuation; this destroys the naively expected symmetry.

Clearly, in the limit as $R \to 0$, all interatomic potentials are Coulombic, and in general they can be written as sums of Coulomb potentials. However, at moderately small distances (on the order of 1 a_0), interatomic potentials are very steeply repulsive, and can be approximated by

$$V(R) \simeq A/R^n$$

with[6] $n \simeq 6$–10. Accordingly, it is reasonable to expect that the analytic behavior of $S(\lambda)$ should be

approximately the same as that which would arise from a highly singular repulsive potential. This assumes that $S(\lambda)$ is stable with respect to changes in the potential in the classically forbidden region near the origin. The WKB theory presented in Sec. III suggests the existence of such stability.

The analytic behavior of $S(\lambda)$ for a singular potential is somewhat simpler than that for a Coulombic potential.[7,8] At the inner turning point, the effective potential

$$\mathcal{U}(R) = V(R) + (L+\tfrac{1}{2})^2/2MR^2$$

is dominated by the strongly repulsive part of $V(R)$, which increases much more rapidly than the centrifugal term. Hence there is no asymmetry in L introduced by the boundary condition at the origin, and it is not difficult[7,8] to show that

$$S(-\lambda) = e^{-2\pi i\lambda} S(\lambda). \tag{5}$$

It follows, of course, that for every pole or zero of S at λ there is a corresponding pole or zero at $-\lambda$. Furthermore, it is known that S can have no poles in the fourth quadrant and no zeros in the first quadrant. It follows from (5) that poles of S will appear only in the first and third quadrants (symmetrically) and zeros only in the second and fourth quadrants. Finally, because $S^*(\lambda^*) = S^{-1}(\lambda)$, the zeros must be complex conjugates of the poles. This behavior is illustrated in Fig. 2.

III. SEMICLASSICAL THEORY FOR REGGE POLES

The formalism for semiclassical calculation of Regge poles was presented by Connor,[4] and in this section we collect the results we need. Connor considered the situation in which the potential contains a barrier, so that for real E and real L there are three real turning points. We supplement his results by considering the case in which the potential does not contain a barrier [Eqs. (12)–(15)].

WKB methods have been used in the past[9-14] to evaluate the behavior of S in the complex k or λ planes, but these studies have generally limited themselves to the effects of the repulsive part of the potential. There have been several studies[9-12] of the high-energy limit of the phase shift for singular potentials, some making use of the analytic continuation of the WKB form of the phase shift

$$\eta = \int_{R_0}^{\infty} [k^2 - 2M\mathcal{U}(R)]^{1/2}\, dR - \int_b^{\infty} (k^2 - \lambda^2/R^2)^{1/2}\, dR$$

into the complex k or λ plane. This formula is valid only in a limited region[13] of the λ plane, because when $\mathrm{Im}\lambda$ gets large additional turning points appear. These additional turning points are very important, because the above formula for the phase shift cannot produce Regge poles. The effects of the additional turning points have been studied by Tiktopoulos,[13] and by Dombey and Jones,[14] who arrived at formulas essentially similar to our Eq. (15). Again they were mainly concerned only with the repulsive part of the potential.

A. Bound States

Consider the effective potentials $\mathcal{U}(R)$ generated from the potential function shown in Fig. 3. For $E<0$, some of the Regge poles represent bound vibrational states, and all of the Regge poles can

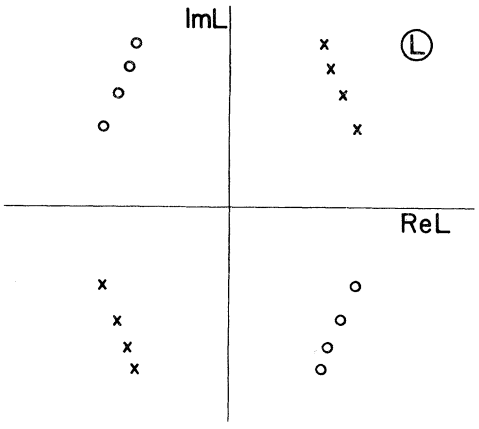

FIG. 2. Symmetry of poles (x) and zeros (0) of the S matrix in the complex λ plane. For each pole at λ_p there is a pole at $-\lambda_p$ and a zero at $\pm\lambda_p{}^*$.

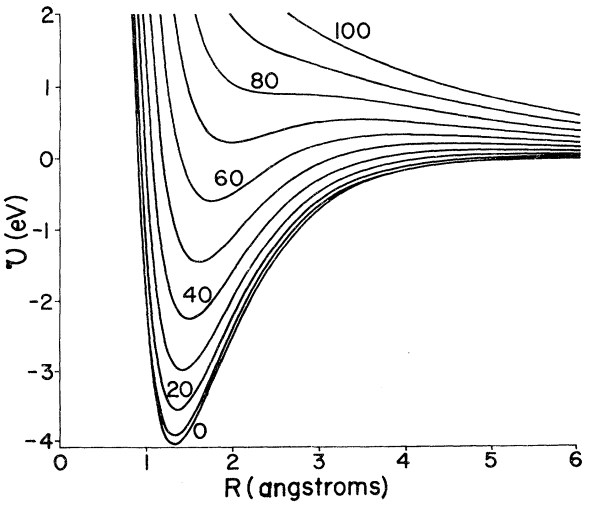

FIG. 3. Effective potentials for H^+-Ar scattering for various values of L from 0 to 100.

be calculated semiclassically from the usual Bohr-Sommerfeld quantization condition

$$-\alpha + (N+\tfrac{1}{2})\pi = 0, \tag{6}$$

where

$$\alpha = \int_a^c P\, dR,$$

$$P = \{2M[E - \mathcal{U}(R)]\}^{1/2}$$

and a and c are the two turning points. In usual bound-state calculations, L is fixed as a positive integer, and one asks at what (discrete) values of E is there a pole of the S matrix, i.e., a bound state. In calculations of Regge poles, however, the question is turned around: First fixing the value of E, one asks, for what value of L is there a pole of the S matrix? The positions of this set of poles $\{L_n(E)\}$ are continuous functions of the energy; when one of these poles is equal to a positive integer, then there is a bound state at that value of L and E. There are, however, additional Regge poles that do not represent bound states. Illustrative calculations will be shown in Sec. IV.

B. Scattering states below the orbiting energy

The effective potential $\mathcal{U}$ for a typical situation is shown in Fig. 4. Points b and d are where $\mathcal{U}(R)$ has its minimum and maximum values, $\mathcal{U}_b$ and $\mathcal{U}_d$. There are three turning points a, c, and e, which will in general be complex if L is complex. We order them by $\mathrm{Re}a \leq \mathrm{Re}c \leq \mathrm{Re}e$, and for $\mathrm{Im}L > 0$, $\mathrm{Im}c < 0$ but $\mathrm{Im}a > 0$ and $\mathrm{Im}e > 0$. Regions I, II, III, and IV are indicated on Fig. 4. Define

$$\alpha = \int_a^c \frac{\mathcal{P}\, dR}{\hbar} \simeq \pi \frac{E - \mathcal{U}_b}{\hbar\omega_b},$$

$$\beta = -\frac{1}{\pi}\int_c^e \frac{\tilde{\mathcal{P}}\, dR}{\hbar} \simeq \frac{E - \mathcal{U}_d}{\hbar\omega_d}, \tag{7}$$

$$\mathcal{P} = \{2M[E - \mathcal{U}(R)]\}^{1/2},$$

$$\tilde{\mathcal{P}} = \{2M[\mathcal{U}(R) - E]\}^{1/2}.$$

Now several cases arise.

1. $E \ll \mathcal{U}_b$; $\alpha \ll 0, \beta \ll 0$

For energies far below the bottom of the well, for L real there is one real turning point e and two complex conjugate turning points (a, c) which are far from the real axis. Let us follow the semiclassical wave function out along the real R axis. First, the wave function increases exponentially with increasing R; around $R = e$ it connects to $\sin[\int_e^R \mathcal{P}\, dR + \frac{1}{4}\pi]$, a superposition of incoming and outgoing waves. But the Regge condition requires that the wave function be asymptotically purely outgoing. Therefore, there can be no Regge poles in this region of E and L.

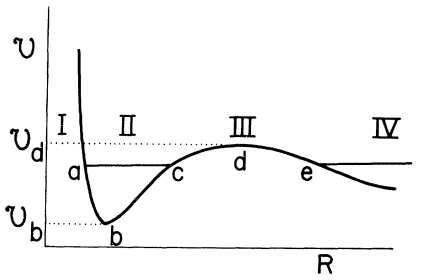

FIG. 4. Qualitative sketch of real part of potential for Regge pole calculation. Two allowed and two forbidden regions are separated by three turning points a, c, e. Points b and d are the minimum and maximum of the potential.

It is at this point that we see that the limiting behavior of $V(R)$ at the origin does not enter our considerations. The WKB connection formula assumes only that $\mathcal{U}(R)$ is approximately linear within a few wavelengths of the turning point, and it does not make special assumptions about other regions. *Within this approximation*, a change in $V(R)$ in the forbidden region far from the turning point has no effect on the wave function in the allowed region. As a consequence, the WKB approximation to the S matrix must have the symmetry property of an S matrix of a singular potential.

2. $E \sim \mathcal{U}_b$; α *small*, $\beta \ll 0$

For energies close to $\mathcal{U}_b$, again, in region I, $u(R)$ must increase exponentially as R increases. We take region II to be those values of R such that $\mathcal{U}(R)$ can be approximated by a quadratic; then $u(R)$ can be written as a superposition of two parabolic cylinder (Weber) functions. The ratio of the coefficients of the two functions is determined by the exponentially increasing behavior in region I. It is then found that $u(R)$ is a superposition of exponentially increasing and decreasing terms in region III; by reversing a connection formula, one can then obtain the wave function in region IV, $R > e$. Finally, imposing the outgoing-wave boundary condition, one obtains a second condition on the ratio of the coefficients. Combining these two conditions leads to the Regge quantization condition:

$$\frac{2(2\pi)^{1/2}}{\Gamma(\frac{1}{2} - \alpha/\pi)\sin\alpha} = i e^{2\pi\beta + 2x}, \tag{8}$$

where

$$2x = (\alpha/\pi)\ln(\alpha/\pi) - (\alpha/\pi).$$

Details are given by Connor.

The derivation can only be valid if the well is essentially parabolic; this normally requires that

a and c be close together, so α will be small. Also the outer turning point must be well away from the inner ones, so $|\beta|$ will be large, and $\mathrm{Re}\beta \ll 0$. It is disturbing that the derivation cannot be made without reversing a connection formula. This is always dangerous, because it is possible that the error in the large solution could become larger than the small solution. However, it is not possible to obtain a purely outgoing wave in region IV unless both the increasing and the decreasing solutions are retained in region III. Perhaps this means that the derivation is valid only if the "large" solution is "not too large"; if so, we would expect to find some deviations from (8) if the barrier is too high or too thick. In that case, however, the widths of the resonances would be so small as to be of little interest in most problems.

Proceeding on the assumption that $|\beta|$ is large, it follows that (8) can be satisfied only where $\Gamma(\frac{1}{2} - \alpha/\pi)$ is large; i.e., only near the poles of the Γ function, at the negative integers. In first approximation, then, we are led again to the Bohr-Sommerfeld condition (6). Expanding the Γ function about its pole, we are led to the approximate condition

$$\alpha - (N+\tfrac{1}{2})\pi = (-i\pi^{1/2}/2\sqrt{2}\,N!)\,e^{2\pi\beta+2x}. \tag{9}$$

3. $\mathcal{V}_b \ll E \ll \mathcal{V}_d; \alpha \gg 0, \beta \ll 0$

If the energy lies between $\mathcal{V}_b$ and $\mathcal{V}_d$, we have three almost real turning points, separating regions I–IV, and the standard linear connection formulas are applied at each. The outgoing-wave boundary condition leads directly to

$$\tan(\alpha+\tfrac{1}{2}\pi) = -\tfrac{1}{4}i\,e^{2\pi\beta}. \tag{10}$$

Again in this derivation it is necessary to reverse a connection formula, and again the procedure cannot be valid unless $|\beta|$ is "large but not too large."

It is easy to show that (9) is equivalent to (10) in the limit of large α. [Equation (10) has additional solutions for $\alpha+\frac{1}{2}\pi \simeq$ (a negative integer), but these are nonphysical because they violate the hypothesis of the derivation, and because Eq. (8) has no such solutions.]

4. $E \sim \mathcal{V}_d; \alpha \gg 0$, β small

For energies close to the top of the barrier, let regions I and II be separated by the inner turning point, $R = a$, and apply the standard WKB connection formula. Assume that in region III the barrier is approximately quadratic, and connect the wave functions in region II to those in IV by examining the asymptotic forms of the Weber (or parabolic cylinder) functions. The resulting semiclassical Regge quantization condition is

$$-\alpha + (N+\tfrac{1}{2})\pi - \tfrac{1}{4}i\beta\pi + \tfrac{1}{2}[\beta - \beta\ln(-\beta)] - \tfrac{1}{2}i\ln[(2/\pi)^{1/2}\cosh\pi\beta\;\Gamma(\tfrac{1}{2}+i\beta)] = 0. \tag{11}$$

This derivation requires that the inner turning point a be well separated from the outer ones, c and e, which must be sufficiently close together that the parabolic connection formulas are valid. (This derivation does not reverse a connection formula.) Equation (11) agrees with (10) in the limit of large negative β, but (11) also holds for energies above the barrier maximum ($\beta > 0$). [To reduce Eq. (11) to Eq. (10), one takes β approximately real, and writes $\Gamma(\frac{1}{2}+i\beta)$ in terms of its magnitude and phase; the former is $(\pi/\cosh\pi\beta)^{1/2}$, and the latter is approximated by Stirling's formula.]

5. Comment on Stokes lines

It is seen that in the above derivation, no use was made of the concept of Stokes lines, or of circumventing the classical turning points on a path in the complex R plane. Nevertheless, it is instructive to consider the positions of the Stokes lines, and their motion as L or E are varied.[15] In Fig. 5(a) are shown the Stokes lines in the complex R plane for L and E real, with $E < \mathcal{V}_d$. The forbidden regions are to the left of a and between c and e.

If L is given a positive imaginary part [Fig. 5(b)], then a and e move into the upper half R plane, and c moves into the lower half plane. The Stokes line that formerly connected c to e here splits into two lines; three lines emanate from each turning point, and no pair of turning points is connected by a Stokes line. The integrals α and β can be evaluated along any curve connecting the turning points, and a straight line is most convenient.

When the energy is raised above $\mathcal{V}_d$ [Fig. 5(c)], the turning points c and e move toward vertical alignment. Finally, when L is again made real [Fig. 5(d)], c and e become complex conjugate points, and a Stokes line again joins them.

C. Scattering states above the orbiting energy

If the energy is above a critical value, orbiting is no longer possible: There is no L for which $\mathcal{V}(R)$ has three real turning points. Such a situation holds for $E \gtrsim 1$ eV in Fig. 3, and the corresponding Stokes lines are shown in Fig. 6. It is seen that $\mathrm{Re}c < \mathrm{Re}a$, and there is now no Stokes line between a and e.

The connection formulas for this situation can be derived by circumventing the turning points on the path indicated, and making use of the following rule: *When crossing a Stokes line clockwise, the coefficient of the small solution is changed by (−i) times*

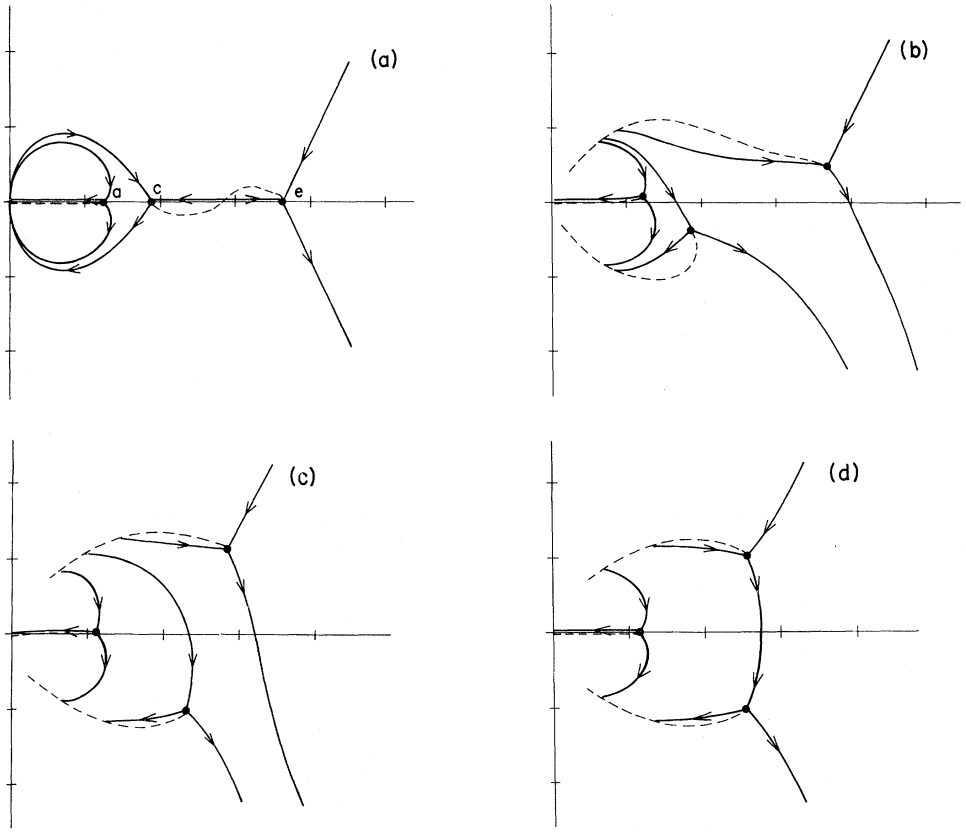

FIG. 5. Stokes lines in the complex L plane when the energy is low enough that orbiting can occur. (a) L is real and $E<\mathcal{V}_d$. There are three real turning points, each with three Stokes lines and a cut (dashed line). (b) L is given a positive imaginary part. Turning points a and e move into the upper half-plane, and c moves into the lower half-plane. The cuts (dashed lines) are now arranged differently, and the Stokes line joining c to e has split into two lines. Turning points are no longer connected by Stokes or anti-Stokes lines. Stokes lines go to the origin on another sheet of the Reimann surface, below the cuts. (c) ReL is lowered so that $E<\mathcal{V}_d$. The lines are qualitatively similar to the case $E<\mathcal{V}_d$, but turning point c is closer to e. (d) L is real, $E>\mathcal{V}_d$. Turning points c and e are complex conjugates, and they are connected by a Stokes line.

the coefficient of the large solution. In Fig. 6, the wave function is exponentially small in region I, and the above lemma gives the usual result

$$\psi_{II} \sim \mathcal{P}^{-1/2} \sin\left(\int_a^R \mathcal{P}\, dR + \tfrac{1}{4}\pi\right) \tag{12}$$

in region II. Passing around e into region III, we cross a Stokes line on which the outgoing $\exp(+i\int_e^R P\, dR)$ is dominant, and therefore the coefficient of the incoming wave changes. The result in region III is

$$\psi_{III} \sim \frac{1}{2i}\, e^{i(\gamma+\pi/4)} \exp\left(i\int_e^R \mathcal{P}\, dR\right)\Big/\mathcal{P}^{1/2} + \tfrac{1}{2}(e^{i(\gamma+\pi/4)} + e^{-i(\gamma+\pi/4)}) \exp\left(-i\int_e^R \mathcal{P}\, dR\right)\Big/\mathcal{P}^{1/2}, \tag{13}$$

where

$$\gamma = \int_a^e \mathcal{P}\, dR. \tag{14}$$

It follows immediately that the poles of S (which occur when the coefficient of the incoming wave vanishes) occur when

$$-\gamma + (N+\tfrac{1}{2})\pi = 0. \tag{15}$$

This formula can also be obtained from (11) by taking the limit $\mathrm{Re}\beta \gg 1, \mathrm{Re}\alpha \gg 1$, and noting that $\gamma = \alpha + i\pi\beta$.

D. Three turning points coincide

There is one important case not covered by the cases above. At the maximum energy for which orbiting is possible, the three turning points coincide. All of the above derivations assume that no more than two turning points are close together, and we do not know of a semiclassical treatment of this three-turning-point problem. We have found that (11) gives plausible results for the positions

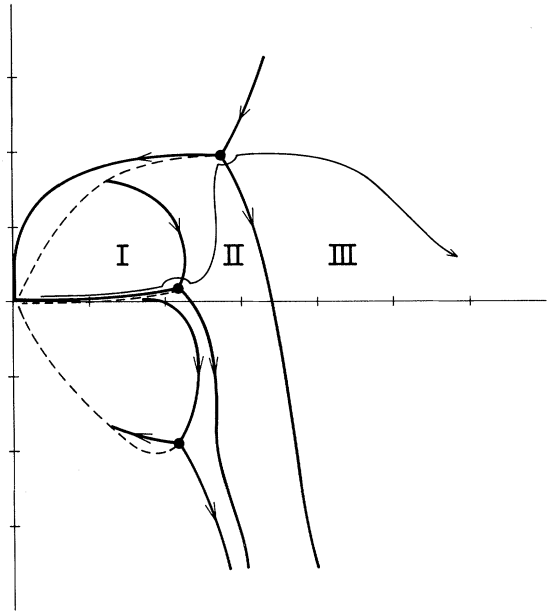

FIG. 6. Stokes lines in the complex L plane when the energy is too high for orbiting to occur. Now c has moved to the left of a, and it no longer is considered in the Regge pole calculation. The fine curve circumventing turning points a and e is the path along which the WKB approximation is made.

of the Regge poles in this case, but a further study of this region, using a direct integration of the Schrödinger equation instead of the semiclassical approximation, would be valuable. Such a study has been carried out by Sukumar and Bardsley,[16] and their results are in complete agreement with ours.

IV. CALCULATIONS

A. Method

The above derivations suggest that different formulas for the locations of the poles of the S matrix should be used for different regions of L and E. In fact, however, the situation is not so complicated. It is not hard to show that Eq. (11) with $N>0$ covers every case: i.e., in appropriate limits, Eq. (11) reduces essentially to Eqs. (6), (8), (10), or (15). Therefore, by finding the roots of Eq. (11) only, we can obtain a good approximation to the correct positions of the Regge poles.

Details of the method are as follows. Having chosen an energy, a first guess is made for the position of the first Regge pole($N=0$). The turning points are obtained by the use of Newton's iterative method (in the complex plane) and the integrals α and β are obtained by numerical integration along a straight line connecting the turning points. Equation (11) and its derivative with respect to L are evaluated (using care to get the correct branch of all the square roots and the logarithm). Finally, the initial guess for L is improved by the complex plane extension of Newton's method. That is, abbreviating Eq. (11) as

$$\Omega(L)=0,$$

then

$$L^{(2)}=L^{(1)}-\frac{\Omega(L^{(1)})}{(d\Omega/dL)_{L^{(1)}}}.$$

The iteration converges if the first guess is close enough, and this is usually no problem. Incrementing N by one unit, the process is repeated to find the set of Regge poles at a given energy, and finally incrementing E, the poles at a higher energy are found. (The whole process takes about 30 sec per pole on the William and Mary IBM 360-50; this is very much less than the time that would be required to find the poles by direct integration of the Schrödinger equation.)

B. Calculated pole positions

Calculations have been performed for the (6,4) potential,

$$V=A/R^6+B/R^4,$$

$$A=2\epsilon\hat{R}^6,\quad B=-3\epsilon\hat{R}^4$$

$$\epsilon=0.160 \text{ hartree}=4.34 \text{ eV},\quad \hat{R}=2.48 \text{ bohr}$$

and for the modified Morse potential,

$$V=\epsilon(e^{2G_1G_2(1-\rho)}-2e^{G_1G_2(1-\rho)}),$$

$$\rho=R/\hat{R},\quad \hat{R}=2.48 \text{ bohr},$$

$$\epsilon=4.04 \text{ eV}=0.1484 \text{ hartree},$$

$$G_1=2.5$$

$$G_2=\begin{cases}1, & \mathrm{Re}\rho<1\\ 0.86, & \mathrm{Re}\rho\geq 1.\end{cases}$$

The modified Morse potential is chosen to reproduce the experimental low-energy scattering data on the H^+-Ar system. The (6-4) potential has approximately the same well depth ϵ and position of the minimum $\hat{R}$, but its well is significantly narrower than that of the Morse potential.

(The modified Morse potential has a discontinuous second derivative at $R=\hat{R}$, and so it is not analytic when continued into the complex plane; it develops a discontinuity at real $R=\hat{R}$. However, this discontinuity is quite small if ImR is small, and it leads to no significant effects. On the other hand, if ImR becomes large, the discontinuity becomes significant and it produces unreliable or meaningless results. ImR will be small on the lines connecting the turning points if ImL is small, i.e., for bound states or narrow resonances.)

For negative energies, many of the poles corre-

spond to bound states; their positions are intuitively obvious, and are shown in Fig. 7. For $L=0$, for the Morse potential, there is a sequence of 25 bound vibrational states, roughly equally spaced in energy, except close to the dissociation limit. As L is increased, each vibrational state moves to a higher energy, and the number of bound states decreases. Since the centrifugal potential is proportional to $(L+\frac{1}{2})^2$, the total energy of each bound state rises from its original value in proportion to $(L+\frac{1}{2})^2$, and the path of each pole in the (E, L) plane is approximately a parabola.

As L continues to increase, the centrifugal barrier becomes high enough to hold quasibound resonance states at positive energies. The most important point to be recognized is that each resonance state is directly correlated with a bound state at a lower value of L; for example, the lowest bound state at $L=0$ remains the lowest bound state for all $L \leq 68$; it becomes the lowest resonance at $L=70$, and it is the last resonance to "disappear" when L is increased further. Thus we see that the same poles of the S matrix correspond to both bound states and resonance states.

The above results are obvious because we are accustomed to fixing L and finding the energies of the bound states and resonances. In the Regge picture, the very same results are described from the opposite point of view: Given E, at what value of L is there a pole of the S matrix? For the bound states and resonances this can also be answered by Fig. 7. At $E \sim -3.9$ eV, there is a pole at $L=0$, and as the energy is increased, L increases. Because of the approximately parabolic shape of the curve, near the bottom, where $dE/dL=0$ or $dL/dE \to \infty$, a small change in energy implies a large change in the L eigenvalue. As the energy continues to increase, the corresponding L eigenvalue increases less rapidly. At an energy of -3.6 eV, a second pole appears at $L=0$ and also moves out the real L axis with increasing E. At E just less than zero, the 25 bound states are now spread out along the real L axis between $L=10$ and $L=65$; their spacing is smallest at large L (~1 unit apart) and largest at small L (perhaps ~5 units apart).

As the energy increases past $E=0$, the poles move into the upper-half L plane. At $E=0.1$ eV, there are seen to be perhaps ten narrow resonances for angular momenta between 40 and 70. As the energy continues to increase these resonances "disappear" one by one. Above the orbiting energy there are no more resonances, and the corresponding poles move away from the physical axis.

The pole trajectories in the complex L plane are shown in Fig. 8 for the Lennard-Jones (6, 4) potential. (This potential well has a slightly greater depth and a smaller width than the modified Morse potential.) We have shown only the poles in the first quadrant. Since the S matrix is symmetric in λ, there is a corresponding set of poles in the third quadrant. At negative energies, we have shown only the trajectory of the first pole. At an energy of -2 eV, the lowest bound state appears at $L=42$ (i.e., at $L=42$, the lowest bound state has an energy of -2 eV) and as the energy is decreased, the corresponding value of L decreases (compare Fig. 7).

At an energy of about -4.2 eV, the lowest state

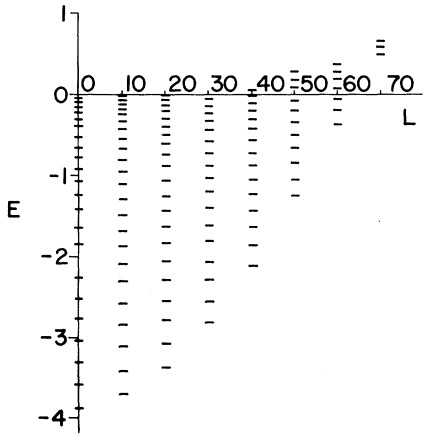

FIG. 7. Energies of bound states and real part of energies of resonances for various values of L for the (modified Morse) potentials of Fig. 3.

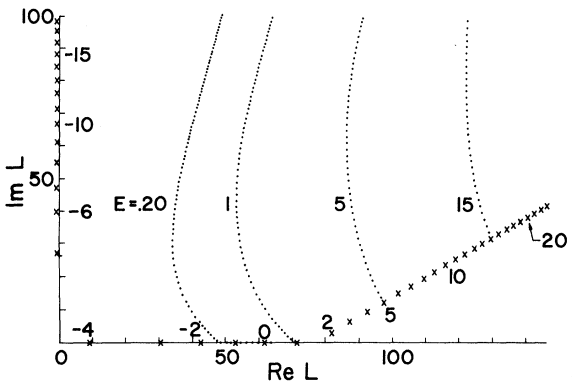

FIG. 8. Regge poles in the complex L plane for various energies. Leading pole (x) is shown for integral values of energy from -18 to $+23$ eV. For $E<-4.3$ eV, this pole lies on the Imλ axis (Re$L=-\frac{1}{2}$). For $-4.3<E<0$ eV it lies on the real L axis, and for $0<E<1.5$ eV it lies barely above the real axis, representing a narrow resonance. At higher energies it moves off into the complex plane. For $E=0.20$, 1, 5, and 15 eV the trailing poles are shown; each dot represents a Regge pole. At $E=0.20$ eV there are ten narrow resonances just above the real axis.

is at $L=0$. If the energy is decreased further, the effective potential cannot support bound states unless the centrifugal term $\lambda^2/2MR^2$ becomes attractive; this can happen for λ purely imaginary, so that the pole moves out the imaginary λ axis ($\mathrm{Re}L=-\frac{1}{2}$). Again because of the dependence on λ^2, the "velocity" of the pole, dL/dE, is large near $|\lambda|=0$ and small for large $|\lambda|$. For example, $\mathrm{Im}L$ goes from zero to 30 when the energy decreases by about 1 eV, but it goes from 70 to 100 only when the energy decreases by about 9 eV.

At a fixed energy (say −2 eV) there is an infinite number of Regge poles. The first eight or so lie on the real L axis, and correspond to the bound vibrational states whose energies lie at 2 eV for various L's (cf. Fig. 7). As before, they are somewhat closer together at large L than at small L. In addition, there is an infinite number of poles extending beside the imaginary axis, at $\mathrm{Re}L=-\frac{1}{2}$. These poles also lie closer together at large $|L|$ than at small $|L|$, but they have no point of accumulation.

When the energy is increased above $E=0$, the poles on the imaginary axis all move away from it very quickly. The poles on the real axis, on the other hand, stay very close to it, since the resonance states have very narrow widths. At $E=0.20$ eV, there are ten narrow resonances, and the rest of the poles lie along a sweeping arc extending essentially vertically in the complex plane. As the energy is raised, the poles peel off the real axis one by one, until at $E=1$ eV for the Lennard-Jones potential there is only one narrow resonance left. As the energy rises further, this pole also moves away from the real axis, and moves along an essentially straight line in the complex plane. Again, as $|\lambda|$ increases, the velocity of the pole decreases. The rest of the poles lie on a smooth curve above the first pole, and they are almost equally spaced on this curve, but slightly closer together as $|\lambda|$ increases. The spacing between adjacent poles can be estimated to within about a factor of 2 by the formula

$$\Delta\lambda \sim M\hat{R}^2\hbar\omega_0/\hbar^2\lambda,$$

where $\hat{R}$ is the equilibrium separation, and $\hbar\omega_0$ is the vibrational energy spacing.

Previous studies[7,8,11,14] have shown that there is an infinite number of poles, that the angle between the Nth pole and the imaginary λ axis goes to zero as $N\to\infty$, but that the real part of λ_N increases without bound as $N\to\infty$. The present calculations are consistent with those results.

C. Calculated residues

In region IV, the wave function may be written as

$$\psi_{\mathrm{IV}}=ce^{ikr-i(l+1/2)\pi/2+i\delta'}+de^{-ikr+i(l+1/2)\pi/2-i\delta'},$$

so that the S matrix may be defined as

$$S=(c/d)e^{2i\delta'}.$$

The parameters c and d are determined by the connection formulas at the turning point $r=e$, and the additional phase δ' is given semiclassically by

$$\delta'=\lim_{R\to\infty}\int_e^R \mathcal{P}(R')\,dR'-\mathcal{P}(\infty)R+\tfrac{1}{2}(l+\tfrac{1}{2})\pi.$$

The formula for d may be expanded in a Taylor series about the zero for d to give the residue

$$R=\frac{1}{2\pi\, d\Omega/dL}\,e^{2\pi\beta-2i\alpha+2i\delta'}.$$

Note that when Eq. (15) is valid for determining the pole position, the residue formula simplifies to

$$R=\frac{-1}{2\pi\, d\Omega/dL}\,e^{2i\delta'}.$$

The residues for the first 20 poles of the Lennard-Jones potential at 5 eV are given in Table I. In calculating δ', we extend R to 40 units to assure convergence. It will be noted that the magnitude of the residues peaks in the region of $N=9$ to 13 and drops steadily thereafter. For $N\geq 90$, the magnitude of the residue is less than 1.

The magnitudes of our tabulated poles are approximately the same as the "exact" residues of

TABLE I. Residues for (6, 4) potential at $E=5$ eV.

Pole	Residue	
	Real part	Imaginary part
1	-0.1344×10^{9}	-0.1194×10^{8}
2	0.1848×10^{10}	0.2258×10^{10}
3	0.6429×10^{9}	-0.2721×10^{11}
4	-0.1103×10^{12}	0.1119×10^{12}
5	0.6229×10^{12}	-0.3031×10^{11}
6	-0.1301×10^{13}	-0.1311×10^{13}
7	-0.2939×10^{12}	0.4200×10^{13}
8	0.6589×10^{13}	-0.4058×10^{13}
9	-0.1050×10^{14}	-0.4943×10^{13}
10	0.8433×10^{12}	0.1462×10^{14}
11	0.1401×10^{14}	-0.7224×10^{13}
12	-0.1038×10^{14}	-0.1045×10^{14}
13	-0.6111×10^{13}	0.1042×10^{14}
14	0.8266×10^{13}	0.3264×10^{13}
15	0.1799×10^{13}	-0.5653×10^{13}
16	-0.3383×10^{13}	-0.1253×10^{13}
17	-0.9617×10^{12}	0.1810×10^{13}
18	0.8282×10^{12}	0.7261×10^{12}
19	0.4779×10^{12}	-0.2812×10^{12}
20	-0.3142×10^{11}	-0.2707×10^{12}
25	0.5281×10^{10}	0.6664×10^{9}
30	-0.8151×10^{8}	-0.5275×10^{8}
40	-0.1760×10^{5}	0.1172×10^{6}

Bardsley and Sukumar, ours generally being 5% larger. The phases also differ. In the peak region, the phases of the Sukumar-Bardsley[16] residues are about 90° larger than ours, but this number is not constant. The reason for the discrepancy is not known; the problem could lie in the numerical methodology, or it could be in an intrinsic limitation on the accuracy of the semiclassical approximations. It should be recognized that the discrepancy is not great in view of the magnitudes of the residues: Logarithmically speaking, the discrepancy is about 10%.

V. DISCUSSION AND CONCLUSIONS

In this paper, we have calculated the positions of the poles of the S matrix—Regge poles—and their residues for a realistic interatomic potential. The semiclassical (JWKB) approximation was used to derive an analog of the Bohr-Sommerfeld quantization condition and this gives us an implicit expression for the pole position. We wish to emphasize the simplicity of this approach: Although the complete theory of Sec. III seems complicated, with different formulas obtained under different assumptions, it is in fact very easy to apply, because one formula, Eq. (11), reduces to all the others in appropriate limits. The poles obtained from this semiclassical formula agree well with the poles obtained by direct integration of the Schrödinger equation.[16]

We now consider the calculation of the scattering amplitude. Noting that the cluster hypothesis reproduces the measured scattering amplitude quite well, we ask if it is possible to obtain an even better result from the actual poles and residues. However, it turns out that a calculational problem involving close cancellations of terms makes a direct calculation unfeasible. We may see this by writing the S matrix as

$$S(\lambda) = 1 + \sum_P \frac{R_P}{\lambda - \lambda_P}$$

and approximating the sum by including only, say, the first 20 poles. The S matrix, which is not guaranteed to be unitary in this representation unless all the poles are included, then has a magnitude of $\sim 10^9$. More poles can, of course, be included but the cancellations which must occur to make $|S| = 1$ require an intrinsic accuracy of more than nine figures; this is not possible in a semiclassical calculation.

Essentially the same conclusion is obtained if one tries to calculate the classical deflection function $\Theta = (2/S)\,(dS/dL)$ from the semiclassical poles and residues. We estimate that some 70–90 terms would be required, and that each residue must be accurate to ±10. Since the largest residues are of order 10^{14}, this would require some 13-figure accuracy, and that is not possible.

In applying the Regge-pole cluster hypothesis to low-energy collision processes, Remler used a product representation to obtain the residues. That representation could be acceptable if the S matrix had a finite number of poles, and no other analytic structure. However, this representation apparently does not apply here, perhaps because there is an infinite number of poles. The residues obtained from the product representation bear no resemblance to the semiclassical residues. The deflection function so obtained is very sensitive to the number of poles considered. If the poles are equally spaced, the series for the deflection function will converge if about a thousand poles are included, but then it will converge to the wrong result.

A different approach to the calculation of the cross section from the Regge poles has been taken by Sukumar and Bardsley. While their approach is effective, it seems to be no less work than direct summation of the partial wave series.

From the above discussion it must not be concluded that the cluster hypothesis is inappropriate. On the contrary, it has been proved to be an accurate and useful tool in the analysis of low-energy scattering data. But it is not clear from the above discussion why the method works so well. The data are well fit with a cluster of poles in the first quadrant (with their symmetric partners in the third quadrant), together with some terms representing the hard core. For H^+Ar scattering at 5 eV, the phenomenological fits[2] require 13 poles clustered at $\lambda = 100.2 + 25.8i$. Our line of poles for the situation begins at about the same value of $\mathrm{Re}\lambda$, but with $\mathrm{Im}\lambda = 12.4$, and the poles move more or less directly away from the real axis, with spacing of about 1.7 units. Eight poles are closer to the real axis than the phenomenological cluster; the rest are farther away. The actual residues are largest for poles 9–13, and decrease quickly thereafter. Thus one might say that the cluster is about where it should be to give a good average to the actual poles. The residues however, are calculated using the product representation, and are not at all close to the actual residues.

The essential reason that the cluster hypothesis works is that it gives a good approximation to the attractive part of the deflection function. The latter has a certain maximum depth (rainbow angle), a certain width, and a general shape that can be precisely reproduced by a pole cluster, which requires only three parameters (N, $\mathrm{Re}\lambda$, $\mathrm{Im}\lambda$) to be described. In other words, the cluster hypothesis provides an effective way of fitting the sorts of deflection functions that one expects in these scattering processes, and therefore it gives

a good approximation to the resulting scattering amplitude.

ACKNOWLEDGMENTS

It is a pleasure to thank E. A. Remler for many discussions. One of us (J. D.) would like to thank Tina Lien for programming assistance. This research was partially supported by NASA and NSF. Finally, we wish to thank J. N. Bardsley and C. V. Sukumar for several conversations concerning their work.

[1]E. A. Remler, Phys. Rev. A 3, 1949 (1971).
[2]S. M. Bobbio, W. G. Rich, R. L. Champion, and L. D. Doverspike, Phys. Rev. A 4, 957 (1971); A 4, 2253 (1971).
[3]A. Sommerfeld, *Partial Differential Equations in Physics* (Academic, New York, 1949).
[4]J. N. L. Connor, Mol. Phys. 25, 1469 (1973); 15, 621 (1968); 23, 717 (1972).
[5]R. G. Newton, *Complex j-plane* (Benjamin, New York, 1964).
[6]I. Amdur and J. E. Jordan, *Molecular Beams*, Vol. X of *Advances in Chemical Physics*, edited by J. Ross (Interscience, New York, 1966).
[7]E. Predazzi and T. Regge, Nuovo Cimento 24, 518 (1962); M. Giffon and E. Predazzi, Nuovo Cimento 33, 1374 (1964).
[8]W. M. Frank, D. J. Land, and R. M. Spector, Rev. Mod. Phys. 43, 36 (1971).
[9]A. Paliov and S. Rosendorff, J. Math. Phys. 8, 1829 (1967).
[10]L. Bertocchi, S. Fubini, and G. Furlan, Nuovo Cimento 35, 599 (1965); 35, 633 (1965).
[11]B. Jaksic and N. Limic, J. Math. Phys. 7, 88 (1966).
[12]N. Limic, Nuovo Cimento 26, 581 (1962).
[13]G. Tiktopoulos, Phys. Rev. 138, B1550 (1965).
[14]N. Dombey and R. Jones, J. Math. Phys. 9, 986 (1968).
[15]A. Z. Patashinskii, V. L. Pokrovskii, and I. M. Khalatnikov, Zh. Eksp. Teor. Fiz. 44, 2062 (1963); 45, 760 (1963) [Sov. Phys.—JETP 17, 1387 (1963); 18, 522 (1964)].
[16]C. V. Sukumar, and J. N. Bardsley, J. Phys. B (to be published).